Recent History of Trends in Vegetation Greenness and Large-Scale Ecosystem Disturbances in Eurasia

Christopher Potter [1*], Vipin Kumar [2], Steven Klooster [3], Ramakrishna Nemani[1]

[1] NASA Ames Research Center, Moffett Field, CA

[2] University of Minnesota, Minneapolis, MN

[3] California State University Monterey Bay, Seaside, CA

[*] Corresponding author

Email: cpotter@mail.arc.nasa.gov

Abstract

Recent patterns of land cover and vegetation dynamics on the Euasian continent have been linked to changes in the global carbon cycle. Our study was conducted to evaluate patterns in a 19-year record of global satellite observations of terrestrial vegetation from the Advanced Very High Resolution Radiometer (AVHRR) as a means to characterize major trends in both vegetation "greenness" and ecosystem disturbance. The fraction absorbed of photosynthetically active radiation (FPAR) by vegetation canopies worldwide has been computed from the AVHRR at a monthly time interval from 1982 to 2000 and gridded at a spatial resolution of 8-km globally. Unlike previous studies of the AVHRR multi-year time series of vegetation dynamics, the 8-km spatial resolution makes it possible to compare disturbance events and greenness trends at the same level of spatial detail. Positive trends in FPAR were detected throughout a major greenbelt of central-eastern Europe starting in the mid-1980s. This Eurasian greenbelt extended in a wide swath over the Urals, into the vicinity of Lake Baykal south of the central Siberian plateau, mainly along a latitude belt from 55° N to 65° N. There was also significantly positive greening in relatively large areas of Great Britain, Italy, Greece, Turkey, the Caucasus, and southern India. Nonetheless, a strong downward trend in the FPAR time series over most of Eurasia was observed by the end of the 1990s. Throughout the 19-year time period, Eurasia was also impacted by many notable droughts and other disturbance events that could have substantially offset decadal carbon gains attributed to satellite-observed greening. Large-scale ecosystems disturbance events were identified in the FPAR time series by locating anomalously low values (FPAR-LO) that lasted longer than 12 consecutive months at any 8-km pixel. We find verifiable evidence of numerous disturbance types across Eurasia, including regional patterns of severe droughts, forest fires, and insect outbreaks.

Keywords: ecosystem disturbance, remote sensing, fire, drought, forests

1. Introduction

Europe's terrestrial sink for atmospheric CO_2 has been estimated as a net uptake flux of between 0.14 and 0.2 Pg C per year (Janssens et al., 2003). Potter et al. (2003a) estimated the potential terrestrial sink for atmospheric CO_2 over the larger Eurasian continental area at between 0.3 and 0.6 Pg C per year since 1988, except during relatively cool temperature periods such as 1991–1992 and 1995–1996 when the Eurasian continental carbon sink was predicted to vary between 0.1 and 0.25 Pg C per year. Although large uncertainties still exist, the mechanisms driving this type of consistent carbon sink flux in terrestrial ecosystems of Eurasia could involve a combination of climate change (warming) and land use transitions (Lucht et al., 2002; Nemani et al., 2003; Zhou et al., 2003).

The overall trend of land cover change in Europe since the 1960s has been a decrease in agricultural land, both arable and grassland, and an increase in reclaimed forest land and urban areas. The forested area in Europe has increased by 10% (15 million hectares) since 1961 due to afforestation of surplus fields and drainage of wetlands. (Lambin et al., 1997). One consequence is that forests have a larger potential than pastures and croplands to sequester atmospheric carbon dioxide (CO_2) over the time scale of a few decades.

Acting to counter climate change and related vegetation growth enhancements, ecosystem disturbances are important sources of CO_2 return to the atmosphere (Schimel et al., 2001). Because major 'pulses' of CO_2 and other trace gases from terrestrial biomass loss can be emitted to the atmosphere during large disturbance events, the timing, location, and magnitude of vegetation disturbance is presently a major gap in understanding global biogeochemical cycles (Pickett and White, 1985; Walker and Willig, 1999; Canadell et al., 2000).

Potter et al (2003b) characterized a large scale ecological disturbance as an event that results in a sustained disruption of ecosystem structure and function, generally with effects that last for time periods longer than a single seasonal growth cycle for native vegetation. Physical

disturbance categories include fires, hurricanes, floods, droughts, and ice storms. Biogenic disturbance categories include the impacts of herbivorous insects, mammals, and pathogens. Anthropogenic disturbance categories include logging, deforestation, drainage of wetlands, clearing for cultivation, chemical pollution, and alien species introductions. Major disturbance events located in the northern latitudes of Eurasia could be associated with seasonal temperature extremes, with close linkages to wildfires and insect outbeaks.

The present study was conducted to evaluate patterns in a 19-year (1982-2000) record of satellite AVHRR observations of vegetation greenness over Eurasia as a means to characterize major trends in land cover and ecosystem disturbance events for the first time at a common spatial resolution of 8-km (image pixel size of about 64 km^2). The fraction absorbed of photosynthetically active radiation (FPAR) by vegetation canopies worldwide has been computed from the National Oceanic and Atmospheric Administration's (NOAA) polar-orbiting AVHRR at a monthly time interval from 1982 to 2000. Like the Normalized Difference Vegetation Index (NDVI), higher FPAR levels observed over the course of a seasonal plant growing cycle indicates denser green leaf cover and (presumably, on average) less disturbance of the vegetation cover, and/or a longer the time period has elapsed since the last major disturbance.

2. Previous Studies of Vegetation Change in Eurasia

Lucht et al. (2002) reported that there has been a "greening" trend in terrestrial ecosystems of northern latitudes, mainly associated with a gradual lengthening of the growing season. This has also been shown by additional evidence such as tree phenology trends (Menzel and Fabian, 1999) and reduced snow cover extent (Groisman et al., 1994) during the past two decades. The trend could not be explained away as an artifact of the methods used to calibrate the extended AVHRR sensor time series compared by Lucht et al. (2002).

Buermann et al. (2003) estimated the year-to-year variations in northern vegetation greenness in relation to the dominant global modes of climate variability, using the AVHRR vegetation greenness, surface temperature, precipitation, and upper air data for the 1982-1998

period. They reported that the El Nino-Southern Oscillation (ENSO) signal is manifested as warmer and greener conditions in North America, Far East Asia, and to some extent in central Europe, while the positive phase of the Arctic Oscillation (AO) signal was associated with enhanced warm and green conditions over large regions in Europe and Asian Russia. In the positive phase of AO, frigid winter air does not extend as far into the middle of the Northern Hemisphere land masses as it would during the negative phase of the oscillation (Thompson and Wallace, 2001). During the mid-1980s and early 1990s, the Arctic Oscillation was mainly in the positive phase. This reduced the number and frequency of days with subzero temperatures or substantial snowfall in the northern mid-latitudes.

In an analysis of global changes in vegetation greenness from 1982-1999, Zhou et al. (2003) reported that AVHRR NDVI generally increased at a regional scale (2^{o} x 2^{o} grid boxes) between the early 1980s and the late 1990s in a swath from central Europe through Siberia to the Aldan plateau. Increasing summer-time temperatures were associated with a notable portion of the interannual increase in NDVI that stretched across the western portion of Eurasia. Variations in regional precipitation amounts did not account for a sizable portion of the variations in NDVI. According to Zhou et al. (2003), an additional explanation for NDVI increases in Europe (east to the Urals) was expansion of forested areas.

Neither Lucht et al. (2002), Buermann et al. (2003), nor Zhou et al. (2003) explored the relative magnitude of these greenness trends at the relatively high resolution of 8-km resolution among sub-areas of the continent, nor did they address the potential impact of ecosystem disturbances on greenness patterns. Our current analyses of the 8-km FPAR time series is intended to fill these gaps, and examine the Eurasian continent at a spatial level of detail wherein both large-scale climate patterns and smaller-scale land cover transitions can be captured. The 8-km AVHRR multi-year time series of vegetation dynamics makes it possible to move beyond single disturbance events to conduct studies of "disturbance regimes". A disturbance regime is defined according to the spatial, temporal, and qualitative nature of disturbance events occurring within any given ecosystem type (Heinselman, 1973). A natural disturbance regime (such as a forest fire cycle) can be described in terms of spatial extent (hectares) and distribution

(patchiness), as well as the frequency and seasonality of its occurrence over time, and its severity or intensity (i.e., the energy released per unit area and time).

Several previous studies have been conducted to quantify carbon emissions from single categories of disturbance, principally biomass burning events, and generally with national or continental levels of resolution. These studies include Kurz and Apps (1999), Houghton et al. (1999), Murphy et al. (2000), Amiro et al. (2001) for portions of North America, Fearnside (1997), Nepstad et al. (1999), Potter et al. (2001) for portions of South America, Scholes et al. (1996), Barbosa et al. (1999) for portions of Africa, Houghton and Hackler (1999) and van der Werf et al. (2004) for portions of Southeast Asia, and Hurst et al. (1994) for Australia. Several studies have dealt with global level effects of deforestation of carbon emissions (Andreae, 1991; Houghton, 1999; Potter, 1999).

3. Data and Analysis Methods

The processing of AVHRR data for vegetation reflectance involved cloud screening and calibration for sensor degradation and intersensor variations. Residual atmospheric effects were minimized by analyzing only the maximum greenness value within each monthly interval (Myneni et al., 2001). These data generally correspond to observations from near-nadir viewing directions and clear atmospheric conditions. The data from April 1982 to December 1984 and from June 1991 to December 1993 were corrected to remove the effects of stratospheric aerosol loadings from El Chichon and Mount Pinatubo eruptions on the FPAR values. As stated previously in Buermann et al. (2002), the wintertime greenness values from 8-km AVHRR data are frequently close to zero at latitudes north of 45^{o} N, largely due to lack of valid wintertime data and low sun angles.

Monthly FPAR greenness values for the land surface have been derived from AVHRR data sets covering the period 1982-2000. This data set was generated using canopy radiative transfer algorithms (Knyazikhin et al., 1998), which are designed to improve vegetation cover products for input to terrestrial carbon flux calculations. These radiative transfer algorithms,

developed for the MODIS (MODerate resolution Imaging Spectroradiometer) aboard the NASA Terra and Aqua satellite platforms, account for attenuation of direct and diffuse incident radiation by solving a three-dimensional formulation of the radiative transfer process in vegetation canopies. Monthly composite data from channels 1 (visible) and 2 (near-infrared) of the AVHRR have been processed according to the MODIS radiative transfer algorithms into a greenness index called FPAR, for the fraction absorbed of photosynthetically active radiation. Monthly FPAR was aggregated over the global land surface from 1-km to 8-km spatial resolution. This aggregation level generates single grid cell (pixel) areas of approximately 6400 ha (1 ha = 10^4 m^2).

Previous studies by Lotsch et al. (2003) have examined the sensitivity of remote sensing-based retrievals of the AVHRR NDVI and FPAR to land cover information used to parameterize vegetation canopy radiative transfer models. A time series of NDVI data from the AVHRR was used in association with extensive site-based training data compiled using Landsat Thematic Mapper (TM) and ancillary map sources. Results showed that retrievals of FPAR proved to be relatively robust to uncertainty in land cover.

3.1 FPAR Trends Analysis

Earth-observing satellites have monitored daily leafy vegetation cover and FPAR on land (also called 'greenness' cover) for more than 20 years (Myneni et al., 1998). Over most of Eurasia, seasonal temperature differences are the principal driver of a yearly oscillating FPAR pattern. The strong seasonal cycle of FPAR (see example in Figure 1) provides a number of repeating attributes that can be tracked on a yearly time interval. We computed the 12-month summed (Jan-Dec) FPAR, along with the annual minimum and annual maximum FPAR values as attributes to characterize changes in the time series from 1982 to 2000.

Linear regression was applied to the time series of annually summed FPAR values for each year 1982 to 2000, as well as to the time series of annual minimum and annual maximum

FPAR values for each year. The slope of the FPAR attribute trend was labeled as either positive or negative. The Pearson Product-Moment correlation coefficient (R^2) was used as a test of significance for these regression results. The 95% confidence level is a $R^2 = 0.2$ for a two-tailed test of significance in these regression results.

3.2 Detection of Major Disturbance Events

Potter et al. (2003b) reported an approach for detection of large-scale ecosystem disturbance (LSEDs) events based on sustained declines in vegetation greenness observed by daily satellite observations. This approach is global in scope, covered more than a decade of analysis, and encompassed all potential categories of major ecosystem disturbance -- physical, biogenic, and anthropogenic – using a consistent method of detection and analysis. The method was based on the 18-year record of global satellite observations of vegetation phenology from AVHRR as a time series to characterize major ecosystem disturbance events and regimes. FPAR of vegetation canopies worldwide was computed at a monthly time interval from 1982 to 1999 and gridded at a spatial resolution of 0.5° latitude/longitude. Potential disturbance events of large extent (greater than a single 8-km pixel area of 6400 ha) were identified in the FPAR time series by locating anomalously low values (FPAR-LO) that lasted longer than 12 consecutive months at any pixel. Disturbance regimes were further characterized by association analysis with historical climate events worldwide.

This FPAR-LO detection approach is based on the concept that leafy vegetation cover is likely the most fragile and therefore perhaps the single most vulnerable biotic component of terrestrial ecosystems to detectable alteration during major disturbance events. Leaf cover burns relatively easily or it can be readily blown down, cut to the ground, or defoliated by herbivores. Leaf litter then decomposes rapidly to blend in with background soil attributes, at least compared to the large woody biomass components of shrub, woodland, and forest ecosystems. It is plausible that any significant and sustained decline in vegetation FPAR observed from satellites represents a disturbance event, a hypothesis we evaluated here using independent records of such disturbance events throughout Eurasia.

The observed FPAR time series at each pixel was first detrended (see example in Figure 1) using a linear adjustment, which is necessary to minimize the possibility that, in cases where there is a gradual but marked increase in monthly FPAR over the 18-yr time series, any potential disturbance events occurring relatively near the end of the series are not overlooked. To remove the dominant seasonal oscillations in vegetation phenology observed throughout the globe, our detrended FPAR time series was subsequently 'deseasonalized' by computing the 12-month running average time series for every pixel location.

An algorithm was next developed to identify any significant and sustained declines in FPAR during the time series.

LSED = IF (FPARsd > 1.7) for >=12 MO_c THEN 1 ELSE 0

where FPARsd is the number of standard deviations below the 18-yr average monthly FPAR, and MO_c is the number of consecutive months in the 18-yr time series. Using a global 0.5° latitude/longitude FPAR data set, the algorithm was tested with a newly compiled data set of majored documented wildfires and cropland production failures worldwide from 1982-1998 and was found to have a sensitivity of successful event detection at disturbance area thresholds of at least 0.1 Mha in the polar zones to 0.3 Mha at the equator (Potter et al., 2003b).

We hypothesized that significant declines in average annual FPAR levels can be defined to be greater than 1.7 standard deviations (SD) below (LO) the 18-yr average FPAR computed for any specific pixel location. A "sustained" disturbance event would be defined as any decline in average annual FPAR levels (at an assigned significance level) that lasts for a temporal threshold value of at least 12 consecutive monthly observations at any specific pixel location. The logic used here is that an actual disturbance involves a sustained decline in FPAR because the structure of the vegetation cover has been severely altered or destroyed during the disturbance event, to a magnitude that lowers FPAR significantly for at least one seasonal growing cycle, after which time regrowth and recovery of the former vegetation structure may permit FPAR to increase again.

It is assumed that fairly common effects of atmospheric interference with the AVHRR channel signals, such as heavy cloud cover or smoke-derived aerosols, would not persist (e.g., as a false disturbance event) in the multi-year time series and thereby generate a FPAR-LO pattern longer than about six months. By design, our disturbance algorithm should be insensitive to heavy cloud cover or smoke effects that occur practically every year during the same season, or only episodically for one or two months at a time. If an interference effect occurs every year at about the same time, it will be eliminated automatically as part of the deseasonalization algorithm. One possible exception to this principle could be persistent atmospheric interference effects generated by major volcanic eruptions, such as the Pinatubo event of late 1991.

While it may be the case that FPAR can vary from year to year during dormant (non-growing) seasons, it is also possible for actual disturbances to occur during the dormant season, such as ice damage or an extremely low snow season. Dormant season events may also affect the quality of the following leaf-out and green-up periods in the growing season. Therefore, we cannot justify excluding the dormant season from our time series analysis. Furthermore, periodic errors in leafless canopy (versus full canopy) estimates of FPAR are not likely to have a major impact on the long-term (19-year) 12-month running mean FPAR, against which we have detected any and all of the FPAR-LO events.

In the use of a one-sided (LO) statistical t-test, rejection of the null hypothesis means that there is no difference between the 19-yr average for the monthly FPAR level and the consistent FPAR-LO level identified in a string of ≥ 12 consecutive time steps. An absolute value SD ≥ 1.7 represents the 95% LO confidence level, SD ≥ 2.0 represents the 97% LO confidence level, and SD ≥ 2.6 represents the 99% LO confidence level (Stockburger, 1998). Since we have first detrended the FPAR time series by linear regression, the resulting data series should more closely approximate a normal distribution. The resulting data series have18 degrees of freedom for tests of significance (19 yr –1 for a one-tailed test).

4. Continental Results from the FPAR Time Series

4.1 Time Series Trends in Greenness

Positive trends in annually summed FPAR ($p < 0.05$) were extensive throughout ecosystems of central and eastern Europe (Figure 2). A greening trend extended over a swath from central Europe over the Urals in the east and ending in the central Siberian plateau. We characterize this temporal FPAR pattern as a contemporary "Eurasian greenbelt". This band of predominantly forested land cover stretches from northern Spain and Portugal in the west, across the entire continent, to Lake Baykal in the east. It extends in the north-south direction from 65° N to 36° N throughout Europe. The band narrows at the southern extreme to about 48° N as it extends from west to east across Asia. Significant FPAR annual greening trends were also observed over relatively large areas of Great Britain, Italy, Greece, Turkey, the Caucasus, and southern India, for which the coefficient of the linear regression line was $R^2 > 0.2$ ($p < 0.05$).

Within this Eurasian greenbelt zone, the annually integrated vegetation FPAR increased significantly, starting in 1985 and continuing through 1990. The greening trend slowed from 1991 to 1994, and then increased markedly again from 1995 to 1997. From 1998 to 2000, the increasing greening trend reversed to become a decreasing phase. Several locations were selected to illustrate details in the greening trend in FPAR across Eurasia. At a location in Great Britain in east-central Scotland near the town of Perth and another location in eastern Germany between Berlin and Leipzig (Figure 3a and 3b), the wintertime seasonal lows in FPAR increased markedly beginning in 1989. Higher than average cold-season greenness explained much of the upward trend during the 1990s at these locations and in south-central Siberia near the town of Tomsk (Figure 3c), where a return of low wintertime greenness patterns were observed in 1998-99. At a more southerly location in Asia, the increasing trend in FPAR in western India (Figure 3d) was spread more evenly over all seasons of the years and did not show a sharp decline at the end of the 1990s.

Significantly negative greening trends were detected in relatively small areas of southern Spain, Kazakhstan, central China, and Southeast Asia. These areas are examined in more detail in the following sections of the paper that deal with effects of extended drought and other

vegetation disturbance agents that may have had repeated negative impacts on FPAR over the two previous decades.

4.2 Ecosystem Disturbance Detection Results

At a level of SD ≥ 1.7 (95% confidence) for definition of disturbance intensity, we can detect 4,032 pixel locations in Europe (west of 50° E longitude) and 10,058 pixel locations in Asia at the threshold of 12 consecutive monthly time steps for FPAR-LO events (Figure 4). For all vegetated land areas of Europe and Asia, the fraction of total land area that had at least one FRAR-LO event was 2.2% and 2.3%, respectively. Summed over 19 years, these pixels together cover a total area of just under 1 million km^2, which, for comparative purposes, is slightly smaller than the entire country area of Egypt. We hypothesize from these results that each of these pixels identified in Figure 4 has been affected to some degree by at least one LSED over the past two decades.

LSED Distribution Patterns

The distribution with latitude of all pixel areas detected at a SD ≥ 1.7 level lasting >12 consecutive months of FPAR-LO shows potential LSED events detected from northern arctic extremes of 78°N, throughout the middle latitudes, and to the continental southern extreme at 15°S in southeast Asia. The distribution among major global vegetation classes (delineated for this study according the 2001 MODIS land cover product from Friedl et al., 2002) of pixel areas from FPAR-LO events (Figure 4) at SD ≥ 1.7 indicates that approximately 45% of all LSED areas in Europe and Asia were located in forested ecosystems (mainly in northern wetland and coniferous-deciduous areas). Approximately 15% were located in savanna and shrubland ecosystems. The remaining 40% of all LSED areas detected in Eurasia were located mostly in grassland and cropland ecosystems.

As discussed briefly by Potter et al. (2003a), our LSED detection method based on FPAR-LO events is well-suited to ecosystems where there is a predominance of perennial woody vegetation cover in the region. Forests and shrublands recover relatively slowly from a sudden loss of green leaf cover, at least in contrast to grasslands and cultivated ecosystems, where a

notable fraction of the green leaf biomass (and hence the FPAR) that is lost during a disturbance can be recovered fairly rapidly through herbaceous sprouting and plant regrowth during the same year as the disturbance event. Nonetheless, the FPAR results from Eurasia indicate that our LSED detection frequency is just as high within grassland and cropland classes as it is within most forested vegetation classes.

Temporal Variations in LSED Events

When viewed in terms of the consecutive monthly time steps for FPAR-LO >12 months, the distribution of total pixel area at SD ≥ 1.7 shows that 95% of the potential LSED coverage had a duration of between 12 and 20 consecutive months for FPAR-LO events (Figure 5). Beginning from the maximum concentration of pixel areas at 13 consecutive months, the decline in area coverage with an increase in the number of consecutive monthly time steps was nearly exponential ($R^2 > 0.90$), out to the maximum value of 36 consecutive months of FPAR-LO.

The distribution according to the start month for pixel areas detected at the SD ≥ 1.7 level of FPAR-LO lasting > 12 consecutive months shows that the periods of highest detection frequency were 1983, 1987-89, 1993, and 1999-2000 (Figure 6). It is conceivable that these time periods of high detection frequency for FPAR-LO events can be verified as coincident with major climate events during the time series. This kind of verification approach follows in a region-by-region examination of the patterns of potential LSED areas shown in Figures 4 and 6.

5. Reconstruction of Regional Ecosystem Disturbance Types

Verification of actual changes in ecosystems due to LSED events must be based on demonstrated relationships between the results shown in Figure 4 and independently confirmed historical events, together with any major climate anomalies in the regions where potential LSED events are detected. In the topic sections that follow, we summarize regional disturbance types chronologically, with focus on documented droughts, heat waves, wildfires, insect outbreaks, cold waves, and blizzards during the 1980s and 1990s.

Certain extreme climate events, such as droughts or cold waves, occur predictably (i.e., during the same season each the year), but are separated by 12 months in two consecutive yearly cycles, and could result in a lower than average FPAR over the period of impact. Hence, it is necessary to expand the definition of an ecological disturbance type to include consecutive years of unfavorable growing season conditions for a given plant cover.

5.1 Droughts and Insect Outbreaks

Dry hot weather events were common throughout the 1982-2000 time period in many countries of Europe, South Asia, and in large portions of China (Table 1). The sources listed in Table 1 are based on summaries of climate reports for the late 20th Century. In a region as large as Eurasia, droughts were reported in practically every year of the 1980s and 1990s in some country of the region.

The first regional drought and heat wave to occur in the 1980s was reported to impact large parts of Southern India, Sri Lanka, and Indonesia in 1983 (Ramakrishna and Rao, 1991). We detected FPAR-LO events from the AVHRR record in each of these regions starting in 1983 and continuing into 1984 in many areas of southeast Asia including northeastern Thailand (Figure 4).

In Europe, the most prominent disturbance event detected after 1984 covered a sizable area of northwestern Scandinavia. Widespread forest damage was reported in Norway during the early 1990s, and was seemingly related to a combination of unfavorable weather, plus attacks by insects and fungi, forest fires, and air pollution (NRMA, 1997). Tree health status in Norway is measured regularly in terms of average crown density and crown color. For spruce, the average crown density decreased from 85 per cent to 79 per cent from 1989 to 1996. For pine, the average crown density remained around 86 per cent during the period 1989 to 1992, but decreased to 83 per cent in 1992 and has remained at that level. In the case of pine, the share of trees in the best crown density class decreased dramatically by as much as 10.1 per cent from 1991 to 1992. A representative example of the yellow-colored areas shown in Figure 4 is plotted

in Figure 7a, indicating a widespread LSED event in northern Scandinavia during this time period. The relatively long duration (>20 months) of the FPAR-LO anomalies in this area of Norway is suggestive of the severity of this forest damage incident.

We detected prominent FPAR-LO disturbance events in China during the periods of 1988-1990 and 1999-2000. Major droughts in northern China have been documented by Shao and Zhaoyinwang (2003) and Zou et al. (2005) during these same periods. Beginning in 1998-99, severe drought extended from Afghanistan, across western Pakistan, Tajikistan, Uzbekistan, Turkmenistan, and western India, as documented by Agrawala et al. (2001). The effects of these severe droughts in central and southern Asian were detected as FPAR-LO anomalies the same time period (Figure 7b).

5.2 Large-Scale Forest Fires

A critical set of historical disturbance events available for verification of FPAR-LO events as LSEDs are well-documented wildfires that burned areas reported to cover tens of thousands of hectares in a single year or growing season. A list of such events was compiled by Potter et al. (2003b) using publications and reports from the global fire literature. The list was not intended to represent an exhaustive set of fire events over the 19-yr period of the FPAR record, but instead is a list of the largest fire events that could be confirmed for their timing of initiation (to within about 3 months) and geographic location (to within approximately 1° latitude and longitude). Selected wildfire areas have been confirmed for timing and location using Landsat and other relatively high resolution satellite images (Arino and Plummer, 1999).

We find that within the Eurasian region, there were at least four major wildfire events that burned at least 5 Mha in single events occurring between 1982 and 2000 (Table 1). Results in Figure 4 confirm that FPAR-LO events were detected during the reported time period for each of these actual wildfires. As an example from the 8-km AVHRR record, the FPAR time series for the eastern Russia forest area between the Amur and Lena rivers (Figure 7c) shows a significant FPAR-LO event (SD ≥ 2.0) during the summer of 1987. In this case, the recovery from fire back to long-term average FPAR required nearly two years.

We detected many more recent disturbance events as FPAR-LO anomalies in Central Asia and the Siberian Plateau, an example of which is shown in Figure 7d. Evidence cited by Kharuk et al. (2003) suggests that extensive insect damage together with wildfires have been triggered by warm winters and summer droughts during the mid to late 1990s in the Boguchan (59° N, 97° 30'E) and Priangar'e (57° 30' N, 94° 30' E) regions of Russia.

6. Discussion

A main objective of this study was to better understand recent patterns of terrestrial ecosystem change throughout Eurasia and to characterize both greening trends and major disturbance events at a common spatial resolution. To this end, we are able to make several inferences on the basis of results from analysis of the 19-yr FPAR time series from AVHRR observations.

A first major inference is that a major shift occurred in both the satellite FPAR observations and wintertime temperatures over the continent the 1980s. During the late-1980s, the Arctic Oscillation shifted to remain mainly in the positive phase through the mid-1990s (Thompson and Wallace, 2001). This generally reduces the number and frequency of days in the northern mid-latitudes with subzero temperatures or substantial snowfall. Anomalously high precipitation occurs from Iceland though Scandinavia during AO positive phases (Hurrell, 1995). Annually integrated FPAR time series for location from Great Britain, Germany, and central Siberia (shown in Figure 3) all show a striking resemblance to decadal AO index anomalies, with peaks in both FPAR and AO time series in 1988-89 and again in 1994-95.

Lucht et al. (2002) showed some of the same temporal patterns in European vegetation growth enhancement (although not in high spatial detail) as we report in the present study of 8-km FPAR trends, with the largest increases in the maximum summer growth at the end of the 1980s and another notable increase after 1994. Independent use of the LPJ model demonstrated that the trends in the AVHRR greenness record are not due to artifacts from the methods used to calibrate

across the AVHRR sensors in the time series. Lucht et al. (2002) instead explained the trends in enhanced greenness by association with temperature warming and longer growing seasons.

Similar results from the CASA biosphere model suggest that surface warming on the Eurasian continent increased net primary production (NPP) during the 1990s at rates that could have temporarily exceeded subsequent losses of CO_2 from ecosystems (Potter et al., 2003a). This could result, at least partially, because production and decomposition of new litterfall from needleleaf trees in the northern latitudes responds to climate warming with a lag-time long enough to desynchronize these component fluxes of net ecosystem carbon fluxes over a 3-5 year time period. It is crucial to mention that losses of carbon from large-scale disturbance events were not included in the continental ecosystem modeling studies cited above.

Moreover, it should be noted that not all areas of Europe showed a significant greening in the late 1980s and mid 1990s. Again in relation to AO, during winters when the index is in the positive phase, anomalously low precipitation frequently occurs over central and southern Europe, the Mediterranean, and the Middle East (Hurrell, 1995). This large-scale rainfall variability associated with AO may explain the absence of positive greening, or even negative FPAR trends, in areas of southern Spain and the southern Mediterranean region (Figure 2).

A second major inference from our results is that the loss of vegetation and soil carbon in areas detected as having experienced at least one large-scale disturbance event between 1982 and 2000 is large enough to substantially offset an cumulative continental sink on the order of 3 Pg C (0.3 Pg C per year sequestered over 10 years). The pixel areas of FPAR-LO events shown in Figure 4 total to about 285,000 km^2 in Europe (west of 50° E longitude) and 643,700 km^2 in Asia. Assuming that above-ground biomass pools of carbon in forests and shrub lands of Eurasia range from 2600-5320 g C m^{-2} (Potter, 1999; Myneni et al., 2001) and herbaceous pools of carbon in temperate grasslands averages 475 g C m^{-2} (Potter, 1999), the total pool size of above-ground biomass at risk in the FPAR-LO pixels shown in Figure 4 could have been as high as 2.76 Pg C.

Complementary evidence for this second major inference comes from the findings of van der Werf, et al. (2004), who estimated that fire emissions of carbon from southeast Asia alone averaged 0.37 Pg C per year over the period of 1997-2001. Addition of the estimated fire emissions from boreal forest ecosystem in northern Asia during this period likely would bring the total source flux to nearly 0.45 Pg C per year. This continental-scale loss of carbon due to fire-related disturbances alone could be sufficient to balance a representative terrestrial ecosystem sink for atmospheric CO_2 for Eurasia of about 0.3 Pg C per year since 1988 (Potter et al., 2003a).

Although the disturbance estimates of carbon emissions described above can add new insights on ecosystem dynamics for the region, there are several notable limitations in the use of global satellite imagery for mapping land cover dynamics. Small-scale logging and partial tree removal activities cannot be detected reliably at a relatively coarse spatial resolution. The same can be said for wildfires smaller than about 10,000 ha of area burned. Flooding along major rivers is likely to be localized in its disturbance impacts, and therefore not detected. Ice storms and localized wind storms seem to fall into this same category of being below the 8-km detection level for AVHRR data (Potter et al., 2005). The implication of these limitations in large-scale disturbance detection is that the carbon emission(s) estimated above could be an underestimate.

In closing, we suggest that the historical AVHRR satellite greenness record holds numerous undiscovered patterns that may change scientific views of continental and global alterations in the land surface over the past 20 years. In Eurasia, a picture is emerging of periodic droughts and wildfires, possibly coupled with herbivorous insect outbreaks, as among the most important causes of ecosystem disturbance in recent times. If global temperatures continues to warm over interior forested areas of the continent, the results presented in this paper may be a useful baseline against which to compare future changes in large-scale disturbance regimes.

Acknowledgments. This work was supported by grants from NASA programs in Intelligent Systems and Intelligent Data Understanding, and the NASA Earth Observing System (EOS) Interdisciplinary Science Program. Thanks to Varun Chandola, Michael Steinbach, and Pang Ning Tan for development of global data analysis tools.

References

Amiro B.D., Todd J.B., Wotton B.M., Logan K.A., Flannigan M.D., Stocks B.J., Mason J.A., Martell D.L., and Hirsch K.G. 2001. Direct carbon emissions from Canadian forest fires, 1959-1999. *Canadian Journal of Forest Research* 31: 512-525.

Agrawala, S., M. Barlow, H. Cullen, and B. Lyon, 2001, *The Drought and Humanitarian Crisis in Central and Southwest Asia: A Climate Perspective*, International Research Institute for Climate Prediction (IRI) Special Report 01-11, Palisades, New York, 24 pp.

Andreae, M.O. 1991. Biomass burning: its history, use, and distribution and its impact on environmental quality and global climate. In: *Global Biomass Burning: Atmospheric, Climactic and Biospheric Implications,* Levine J.S., editor., New York: MIT Press. p. 3-21.

Arino, O., Plummer S. 1999. Along Track Scanning Radiometer World Fire Atlas: Validation of The 1997-98 Active Fire Product. IGBP Report.

Barbosa, P.M., Grégoire J.-M., Stroppiana D., and Pereira J.M.C., 1999. An assessment of fire in Africa (1981-1991): Burnt areas, burnt biomass and atmospheric emissions. *Global Biogeochemical Cycles*, 13, 933-950.

Buermann, W., Y. Wang, J. Dong, L. Zhou, X. Zeng, R. E. Dickinson, C. S. Potter, and R. B. Myneni, 2002, Analysis of a multiyear global vegetation leaf area index data set, *J. Geophys. Res.,* 107(D22), 4646, doi:10.1029/2001JD000975.

Buermann, W., B. Anderson, C. J. Tucker, R. E. Dickinson, W. Lucht, C. S. Potter and R. B. Myneni, 2003. Interannual co-variability in northern hemisphere air temperatures and greenness associated with ENSO and AO, *J. Geophys. Res.*, 108, NO. D13, 4396, doi:10.1029/2002JD002630.

Cahoon, D. R., Jr., J. S. Levine, W. R. Cofer III, J. E. Miller, G.M. Tennille, T. W. Yip, and B. J. Stocks, 1991. The great Chinese fire of 1987: A view from space. In J. S Levine (ed.), *Global Biomass Burning: Atmospheric, Climatic, and Biospheric Implications*. MIT Press, Cambridge, Mass.

Cahoon, D.R., B.J. Stocks, J.S. Levine, W.R. Cofer, and J.M. Pierson. 1994. Satellite analysis of the severe 1987 forest fires in northern China and southeastern Siberia. *J. Geophys. Res.,* **99**, 18627-18638.

Canadell JG, Mooney HA, Baldocchi, DD, Berry JA, Ehleringer JR, Field CB, Gower ST, Hollinger DY, Hunt JE, Jackson RB, Running SW, Shaver GR, Steffen W, Trumbore SE, Valentini R, Bond BY. 2000. Carbon metabolism of the terrestrial biosphere: a multi-technique approach for improving understanding. *Ecosystems,* 3: 115-130.

Estrela, T., M, Menéndez, M. Dimas, C. Marcuello, G. Rees, G. Cole, K. Weber, J. Grath, J. Leonard, N. Bering Ovesen, J. Fehér, V. Consult, 2001, *Sustainable Water Use in Europe*, Part 3. Extreme hydrological events: floods and droughts, Environmental issue report No 21. European Environment Agency, Copenhagen, 84 pp.

Fearnside P.M., 1997. Greenhouse gases from deforestation in Brazilian Amazonia: Net committed emissions. *Climatic Change,* 35: 321–360.

Friedl M.A., McIver D.K., Hodges J.C.F., Zhang X.Y., Muchoney D., Strahler A.H., Woodcock C.E., Gopal S., Schneider A., Cooper A., Baccini A., Gao F., and Schaaf C., 2002, Global land cover mapping from MODIS: algorithms and early results. *Remote Sensing of Environment,* 83: 287-302.

Groisman, P. Y., T. R. Karl, and R. W. Knight, 1994. Observed impact of snow cover on the heat balance and rise of continental spring temperatures, *Science,* 263, 198.

Heinselman, M.L., 1973, Fire in the virgin forests of the Boundary Waters Canoe Area, Minnesota. *Quaternary Research*, 3: 329-382.

Hoffmann, A. A., L. Schindler, and J. G. Goldammer, 1999, Aspects of a Fire Information System for East Kalimantan, Indonesia. Proceedings of the 3rd International Symposium on Asian Tropical Forest Management, Samarinda, East Kalimantan, Indonesia, 20-23 September 1999.

Houghton, R.A., Hackler J.L., and Lawrence K.T. 1999. The U.S. carbon budget: Contributions from land-use change. *Science,* 285: 574-579.

Houghton, R.A. 1999. The annual net flux of carbon to the atmosphere from changes in land use 1850–1990. *Tellus,* 51B: 298–313.

Houghton, R.A. and Hackler J.L., 1999. Emissions of carbon from forestry and land-use change in tropical Asia. *Global Change Biol.*, 5: 481–492.

Hurrell, J. W., 1995. Decadal trends in the North Atlantic Oscillation regional temperatures and precipitation, *Science*, 269, 676-679.

Hurst, D.F., Griffith D.W.T., and Cook G.D., 1994. Trace gas emissions from biomass burning in tropical Australian savannas. *J. Geophys. Res.*, 99: 16,441-16,456.

Janssens I., A. Freibauer, P. Ciais, P. Smith, G.-J. Nabuurs, G. Folberth, B. Schlamadinger, R.W.A. Hutjes, R. Ceulemans, E.D. Schulze, R. Valentini, and A.J. Dolman, 2003. Europe's biosphere absorbs 7 to 12% of European anthropogenic carbon emissions. *Science* 300, 1538-1542.

Kharuk, V. I., K.J. Ranson, V.V. Kuz'michev, and S.T. Im, 2003, Landsat-based analysis of insect outbreaks in southern Siberia, *Can. J. Remote Sensing*, 29, 286-297.

Knyazikhin, Y., Martonchik J.V., Myneni R.B., Diner D.J., and Running S.W. 1998. Synergistic algorithm for estimating vegetation canopy leaf area index and fraction of absorbed photosynthetically active radiation from MODIS and MISR data. *J. Geophys. Res.*, 103: 32,257-32,276.

Kurz, W.A. and Apps M.J. 1999. A 70-yr retrospective analysis of carbon fluxes in the Canadian forest sector. *Ecological Applications,* 9: 526-547.

Lambin, E., G. Fischer, J. Jäger and X. Baulies, 1997, Conference Proceedings, *Land Use and Land Cover Change In Europe*, Electronic report prepared for the EC DG XII/D (Environment and Climate Programme) Land Use Land Cover Change Group. http://www.geo.ucl.ac.be/LUCC/publications/reportseries/series2/.

Lotsch, A., Y. Tian, M. A. Friedl, and R. B. Myneni, 2003, Land cover mapping in support of LAI and FPAR retrievals from EOS-MODIS and MISR: Classification methods and sensitivities to errors, *Int. J. Remote Sensing*, 24, 1997-2016.

Lucht, W., Prentice I.C., Myneni R.B., Sitch S., Friedlingstein P., Cramer W., Bousquet P., Buermann W., and Smith B., 2002, Climatic control of the high-latitude vegetation greening trend and Pinatubo effect. *Science*, 296, 1687-1689.

Menzel, A. and P. Fabian. 1999. Growing season extended in Europe. *Nature*, 397: 659.

Murphy, P.J., Mudd J.P., Stocks B.J., Kasischke E.S., Barry D., Alexander M.E., and French N.H.F. 2000. Chapter 15: Historical Fire Records in the North American Boreal Forest. In:

Fire, Climate Change, and Carbon Cycling in the Boreal Forests. Kasischke E.S. and Stocks B.J, editors. New York: Springer-Verlag.

Myneni, R,B,, Tucker C,J,, Asrar G,, and Keeling C.D. 1998. Interannual variations in satellite-sensed vegetation index data from 1981 to 1991. *J. Geophys. Res.,* 103: 6145-6160.

Myneni, R. B., J. Dong, C. J. Tucker, R. K. Kaufmann, P. E. Kauppi, J. Liski, L. Zhou, V. Alexeyev, and M. K. Hughes, 2001, A large carbon sink in the woody biomass of Northern forests, *PNAS*, 98, 14784–14789.

Nemani, R.R., C.D. Keeling, H. Hashimoto, M. Jolly, S.W. Running, S.C. Piper, C.J. Tucker and R. Myneni. 2003. Climate driven increases in terrestrial net primary production from 1982 to 1999. *Science,* 300, 1560-1563.

Nepstad, D.C., Veríssimo A., Alencar A., Nobre C., Lima E., Lefebvre P., Schlesinger P., Potter C., Moutinho P., Mendoza E., Cochrane M., and Brooks V. 1999. Large-scale impoverishment of Amazonian forests by logging and fire. *Nature,* 398: 505-508.

Norwegian Royal Ministry of Agriculture (NRMA), 1997, The Norwegian Forest and Forest Protection Act, ISBN 82-504-1175-7, Oslo, Norway.

Pickett S.T.A. and White P.S. 1985. The Ecology of Natural Disturbance as Patch Dynamics. New York: Academic Press.

Potter, C,S. 1999. Terrestrial biomass and the effects of deforestation on the global carbon cycle. *BioScience*, 49: 769-778.

Potter, C,S, Klooster S.A., and Brooks V. 1999. Interannual variability in terrestrial net primary production: Exploration of trends and controls on regional to global scales. *Ecosystems,* 2: 36-48.

Potter, C.S., Brooks-Genovese V., Klooster S.A., Bobo M., and Torregrosa A. 2001. Biomass burning losses of carbon estimated from ecosystem modeling and satellite data analysis for the Brazilian Amazon region. *Atmospheric Environment,* 35: 1773-1781.

Potter, C., Klooster S., Myneni R., Genovese V., Tan P., Kumar V. 2003a. Continental scale comparisons of terrestrial carbon sinks estimated from satellite data and ecosystem modeling 1982-98. *Global and Planetary Change,* 39: 201-213.

Potter, C., P. Tan, M. Steinbach, S. Klooster, V. Kumar, R. Myneni , V. Genovese, 2003b, Major disturbance events in terrestrial ecosystems detected using global satellite data sets. *Global Change Biology*, 9 (7), 1005-1021.

Potter C., Tan P., Steinbach M., Kumar V., Kucharik C., Klooster S., Genovese V., Cohen W., and Healey S., 2005. Recent history of large-scale ecosystem disturbances in North America derived from the AVHRR satellite record. *Ecosystems,* 8(7), 808-822.

Ramakrishna, Y.S. and Rao, A.S. 1991. *Incidence and Severity of Droughts in the Indian Arid Zone and their Impact on Productivity from Agricultural and Pasture Lands*. Indo-Soviet ILTP Meeting on Ecology of Arid Zones and Control of Desertification. Central Arid Zone Research Institute. Jodhpur.

Schimel D., House J., Hibbard K., Bousquet P., Ciais P., Peylin P., Apps M., Baker D., Bondeau A., Brasswell R., Canadell J., Churkina G., Cramer W., Denning S., Field C., Friedlingstein P., Goodale C., Heimann M., Houghton R.A., Melillo J., Moore III B., Murdiyarso D., Noble I., Pacala S., Prentice C., Raupach M., Rayner P., Scholes B., Steffen W., and Wirth C. 2001. Recent patterns and mechanisms of carbon exchange by terrestrial ecosystems, *Nature,* 414: 169-172.

Scholes, R.J., Kendall J., and Justice C.O. 1996. The quantity of biomass burned in southern Africa. *J. Geophys. Res.*, 101: 23,667-23,676.

Shao, X. and H. Zhaoyinwang, 2003, Interbasin transfer projects and their implications : A China case study, *Intl. J. River Basin Management*, 1, 5–14.

Stockburger, D.W. 1998. Introductory Statistics: Concepts, Models, And Applications, WWW Version 1.0, http://www.psychstat.smsu.edu/sbk00.htm.

Thompson, D. W. J., and J. M. Wallace, 2001, Regional climate impacts of the Northern Hemisphere annular mode. *Science*, 293, 85-89.

Tilman D. 1985. The resource-ratio hypothesis of plant succession. *American Naturalist,* 125: 827-852.

van der Werf, G.R., J.T. Randerson, G.J. Collatz, L. Giglio, P.S. Kasibhatla, A. Arellano, S.C. Olsen, and E.S. Kasischke, 2004. Continental-scale partitioning of fire emissions during the 97/98 El Nino, *Science*, 303, 73-76.

Walker, L.R. and Willig M.R., 1999. editors. Ecology of Disturbed Ground, Amsterdam: Elsevier.

Zhou, L., R. K. Kaufmann, 1 Y. Tian, R. B. Myneni, and C. J. Tucker, 2003, Relation between interannual variations in satellite measures northern forest greenness and climate between 1982 and 1999, *J. Geophys. Res.*, 108, doi:10.1029/ 2002JD002510.

Zou, X., P. Zhai, and Q. Zhang, 2005, Variations in droughts over China: 1951–2003, *Geophys. Res. Lett.,* 32, L04707, doi:10.1029/ 2004GL021853.

Table 1. Summary of recent drought events in Europe and Asia (Agrawala et al., 2001; Estrela et al., 2001; Ramakrishna and Rao, 1991; Shao and Zhaoyinwang, 2003; Zou et al., 2005)

1983	SE Asia	Severe drought in Southern India, Sri Lanka, Indonesia
1984	Northern and eastern UK	Dry spring and summer.
1986-1988	China	Severe drought
1987	India	Drought resulting in major losses of crop production
1988–92	Most of Europe (southern England to the Mediterranean)	High summer temperatures and above-average winter temperatures with reduced snowfall; Severe summer drought in north-east Germany in 1992, with crop production reduced by 22%
1990	China	Severe drought
1990–95	Spain, Portugal	Prolonged drought across all of Spain except north coast; Most intense between September 1994 and August 1995
1992–93	Bulgaria, Hungary	Very hot dry summer in 1992, continued with below-average rainfall to October 1993; Low soil moisture in Bulgaria causing severe loss of agricultural production; Worst drought in the Russia for 100 years
1995	Ireland and UK, Norway, Sweden	Hot dry summer and autumn; Low temperatures and little winter snow in Nordic countries
1996	Bulgaria	Hot dry summer across whole country
1997	Germany, France, Ireland, Portugal, UK, China, SE Asia	Very low rainfall throughout Europe; Severe drought in China's Yellow River basin, Thailand, Indonesia, Malaysia, Korea,
1999-2001	Central and Southwest Asia	Severe drought in Iran, Afghanistan, western Pakistan, Tajikistan, Uzbekistan, Turkmenistan, western India, and northern China
1999	Finland	Hot dry summer in southern Finland; Low water levels both in rivers and groundwater formations

Table 2. List of major forest wildfires on record for Eurasia in the 1980s and 1990s.

Year	Location	Area Burned (Mha)	Lat Lon	Available References
1982 and 1983	East Kalimantan, Indonesia	5	0 N 117 E	(Hoffmann et al., 1999)
1987	Russia-China [a]	6-11	51 N 127-128 E	(Cahoon et al. 1991 and 1994)
1996 and 1997	Mongolia	11	46-50 N 100-110 E	
1997	Kalimantan and Sumatra, Indonesia *	9	0-4 S 110-115 E 0-4 S 105 E	(Hoffmann et al.,1999)

[a] In Da Hinggan-Dzhagdy Mountains coniferous forests; fire destroyed the town of Xilinji in Russia east of Lake Baikal between the Amur and Lena rivers.

[b] Additional sources:

European Space Agency Earth Watching Fires Archive (Biasutt and Marchetti, 1996)
ftp://earth1.esrin.esa.it/pub/ew/fires/

* Fire location has been confirmed using Landsat and ATSR (Along Track Scanning Radiometer) satellite images (Arino and Plummer, 1999).

Figure Captions

Figure 1. FPAR–LO event beginning in 1994 in Norway. Top panels are original (raw) FPAR values, scaled 0-256, and bottom panels are the deseasonalized FPAR anomalies in units of standard deviation (SD) in the12-month moving average. Dashed vertical lines show the longest consecutive period of anomalously LO monthly values. Owing to the use of a moving average, the apparent start time of the FPAR-LO events shown in the bottom panels may be up to 12-months shifted from the documented timing of the disturbance event. Latitude is shown in decimal degrees N (+) and S (-), and longitude in decimal degrees W (-) and East (+).

Figure 2. Time series trends in Europe and Asia from linear regression of annual summed FPAR for the years 1982 to 2000. Yellow-orange pixels are labeled as areas that have increased significantly *(p* < 0.05), whereas blue pixels are labeled as areas that have decreased significantly *(p* < 0.05).

Figure 3. Time series trend results at selected sites in Europe and Asia from linear regression of annually summed FPAR for the years 1982 to 2000. Raw FPAR values are shown in the upper panels; Least sum of squares linear regression line is shown with annually summed FPAR series in lower panels. (a) East-Central Scotland near the town of Perth, (b) eastern Germany between Berlin and Leipzig, (c) south-central Siberia near the town of Tomsk, (d) western India. . Latitude is shown in decimal degrees N (+) and S (-), and longitude in decimal degrees W (-) and East (+).

Figure 4. Distribution throughout Europe and Asia of 8-km pixels as the first month and year for FPAR-LO disturbance events lasting >12 consecutive months within the time series 1982-2000.

Figure 5. Distribution according to consecutive monthly time steps of land area detected with at least one FPAR-LO event in the time series 1982-2000.

Figure 6. Distribution according to start month of land area detected with at least one FPAR-LO event in the time series 1982-2000.

Figure 7. (a) FPAR–LO event in Norway from 1992-1993, showing suspected climate and pollution impacts on vegetation greenness, (b) FPAR–LO event in India in 1998-99, showing reported drought and heat wave impacts on vegetation greenness, (c) FPAR–LO event in eastern Russia in 1987 showing reported forest fire impacts on vegetation greenness, (d) FPAR–LO event on the Siberian Plateau in 1999 showing suspected fire and insect outbreak impacts on vegetation greenness. Data presentation in panels is described as in Figure 1.

Figure 1. FPAR–LO event beginning in 1994 in Norway. Top panels are original (raw) FPAR values, scaled 0-256, and bottom panels are the deseasonalized FPAR anomalies in units of standard deviation (SD) in the12-month moving average. Dashed vertical lines show the longest consecutive period of anomalously LO monthly values. Owing to the use of a moving average, the apparent start time of the FPAR-LO events shown in the bottom panels may be up to 12-months shifted from the documented timing of the disturbance event. Latitude is shown in decimal degrees N (+) and S (-), and longitude in decimal degrees W (-) and East (+).

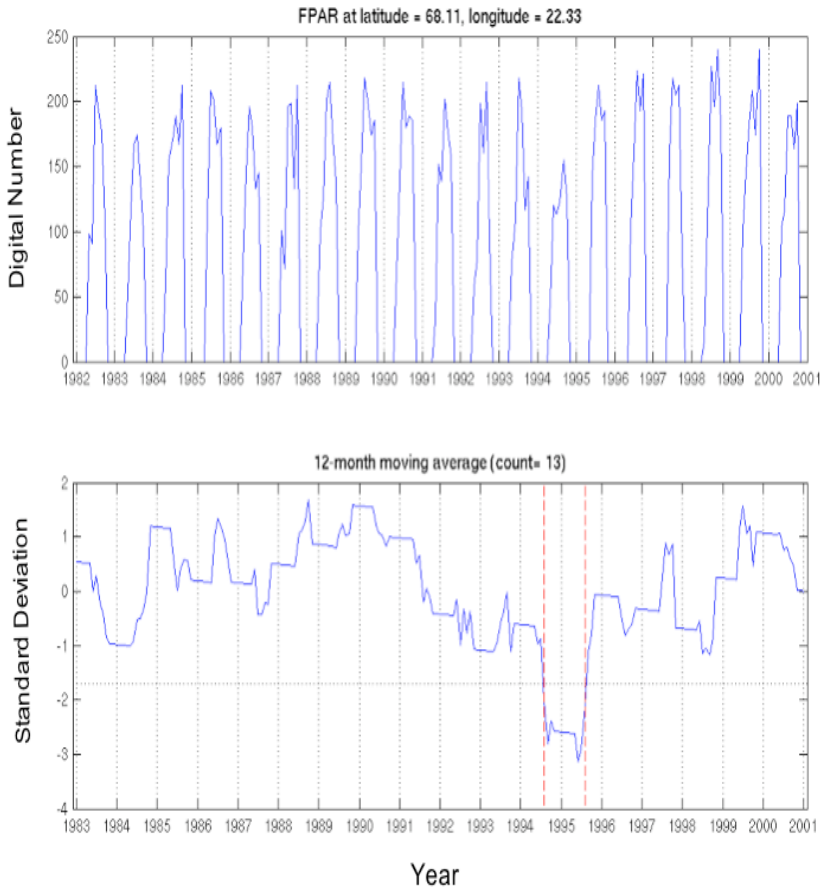

Figure 2. Time series trends in Europe and Asia from linear regression of annual summed FPAR for the years 1982 to 2000. Yellow-orange pixels are labeled as areas that have increased significantly ($p < 0.05$), whereas blue pixels are labeled as areas that have decreased significantly ($p < 0.05$).

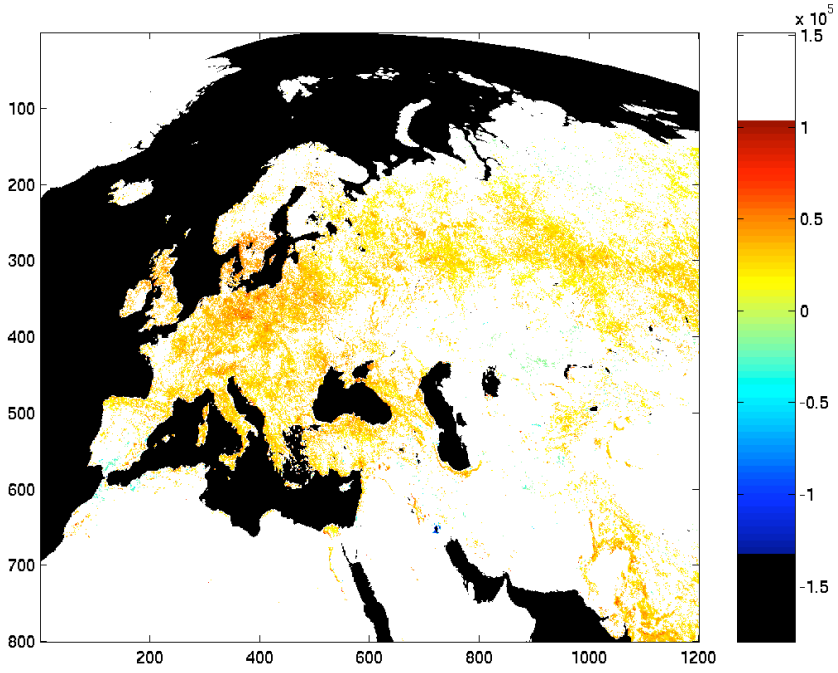

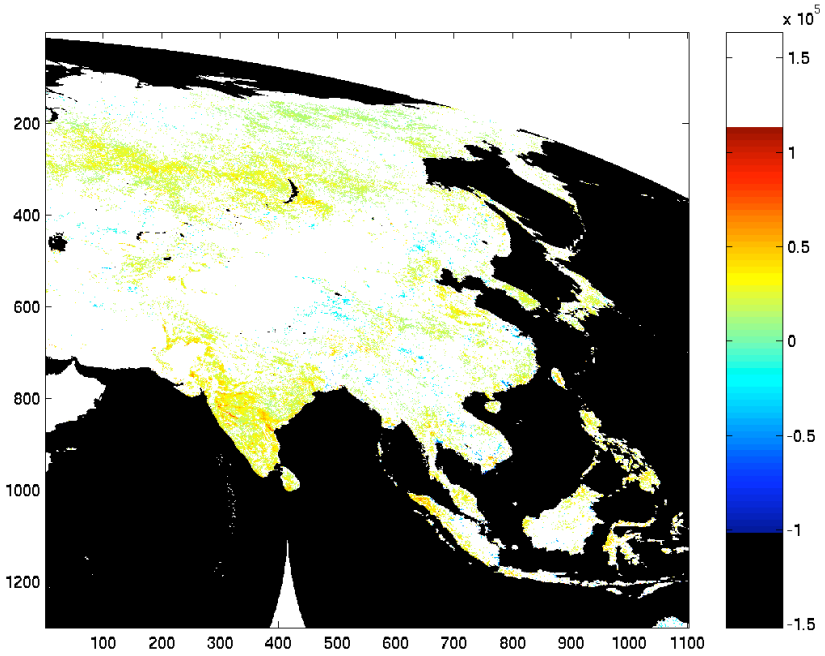

Figure 3. Time series trend results at selected sites in Europe and Asia from linear regression of annually summed FPAR for the years 1982 to 2000. Raw FPAR values are shown in the upper panels; Least sum of squares linear regression line is shown with annually summed FPAR series in lower panels. (a) East-Central Scotland near the town of Perth, (b) eastern Germany between Berlin and Leipzig, (c) south-central Siberia near the town of Tomsk, (d) western India. Latitude is shown in decimal degrees N (+) and S (-), and longitude in decimal degrees W (-) and East (+).

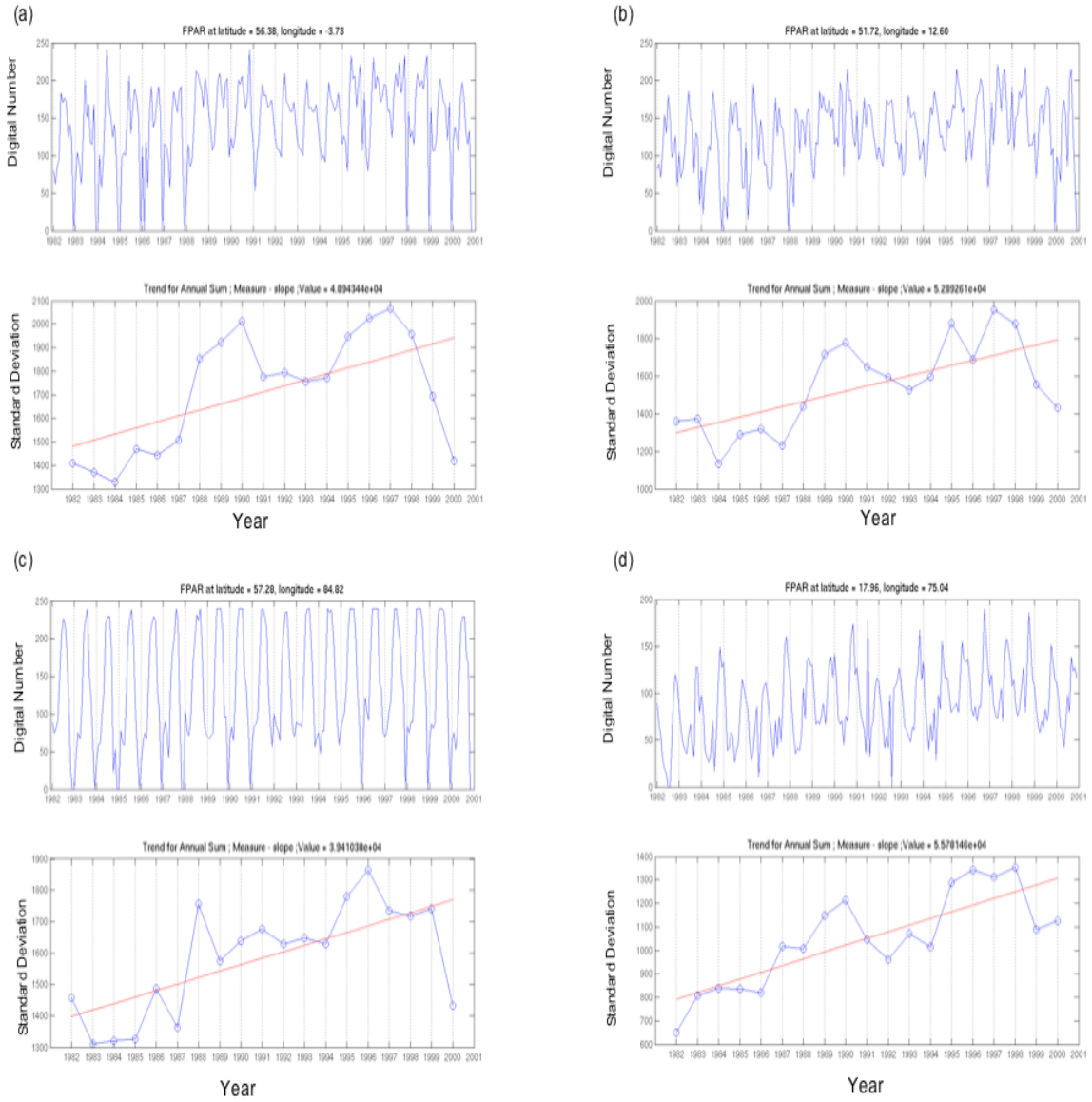

Figure 4. Distribution throughout Europe and Asia of 8-km pixels as the first month and year for FPAR-LO disturbance events lasting >12 consecutive months within the time series 1982-2000.

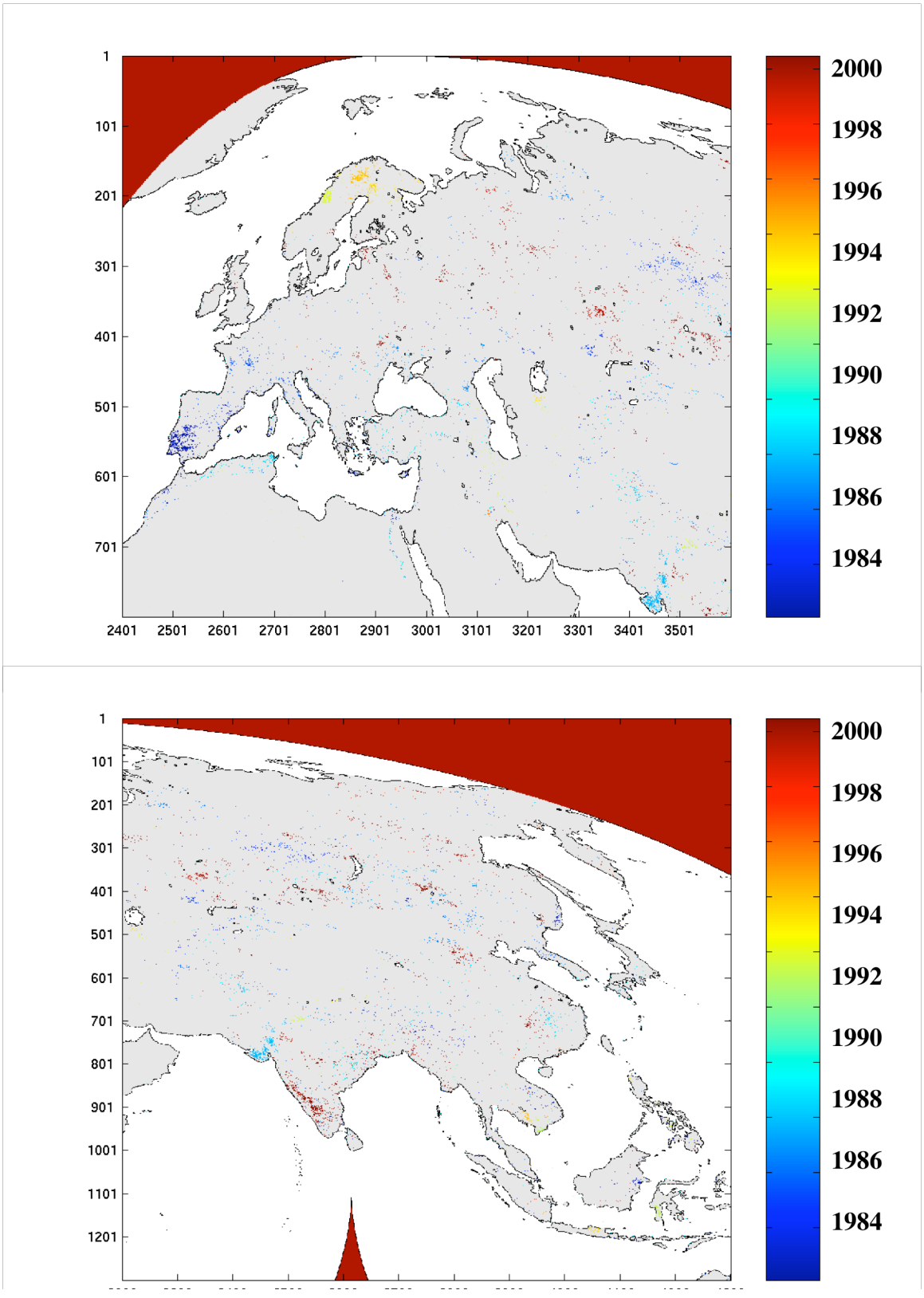

Figure 5. Distribution according to consecutive monthly time steps of land area detected with at least one FPAR-LO event in the time series 1982-2000.

Europe

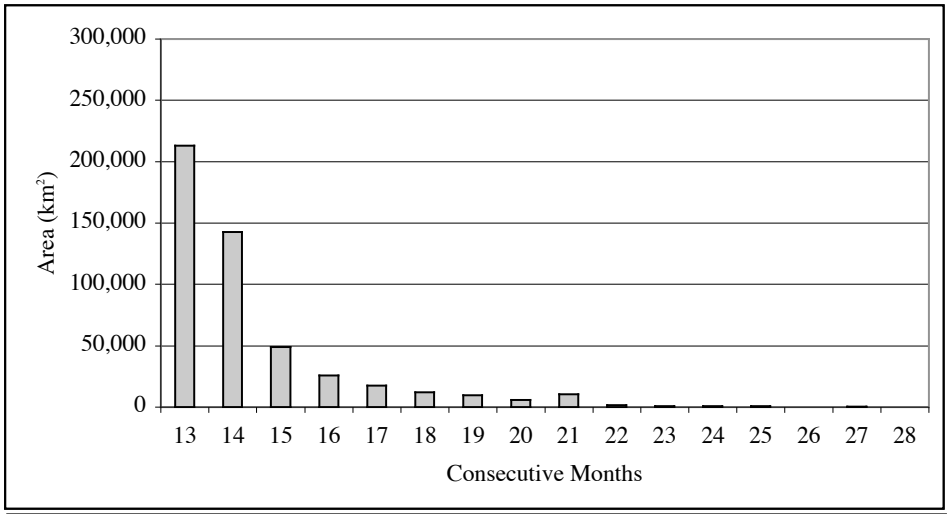

Asia

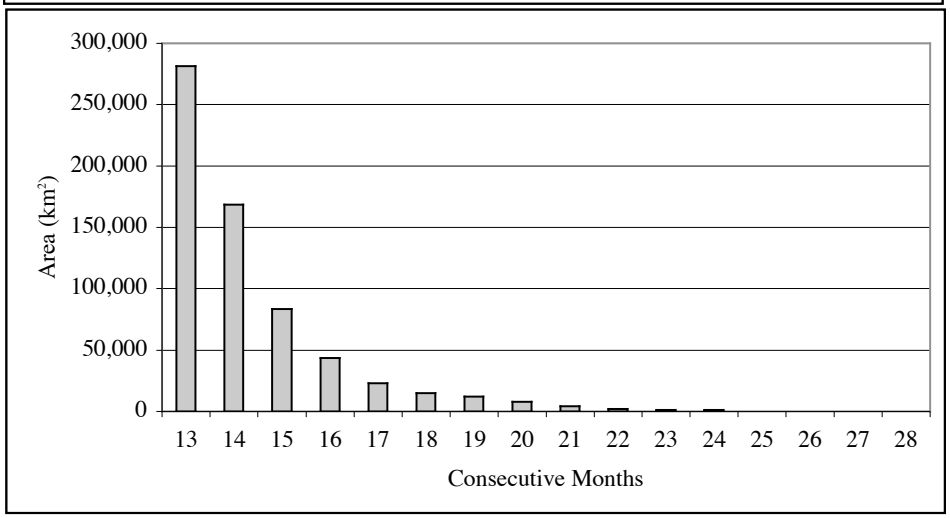

Figure 6. Distribution according to start month of land area detected with at least one FPAR-LO event in the time series 1982-2000.

.

Europe

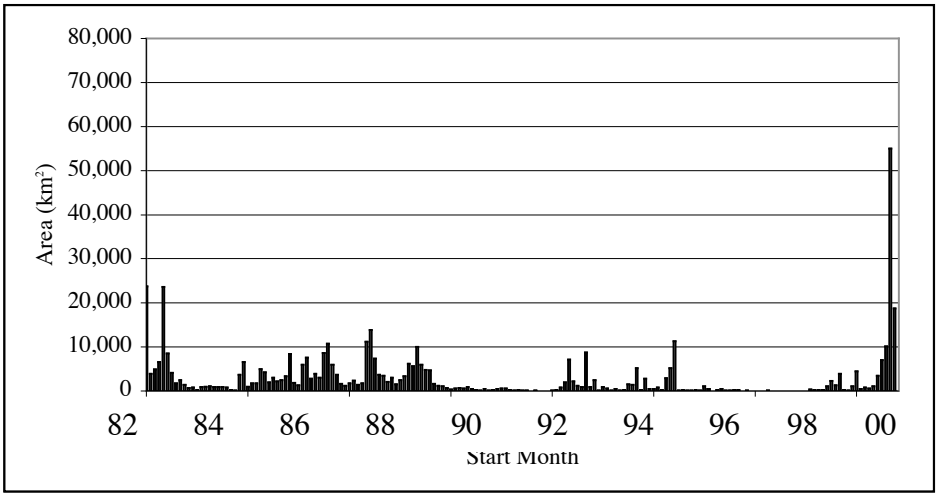

Asia

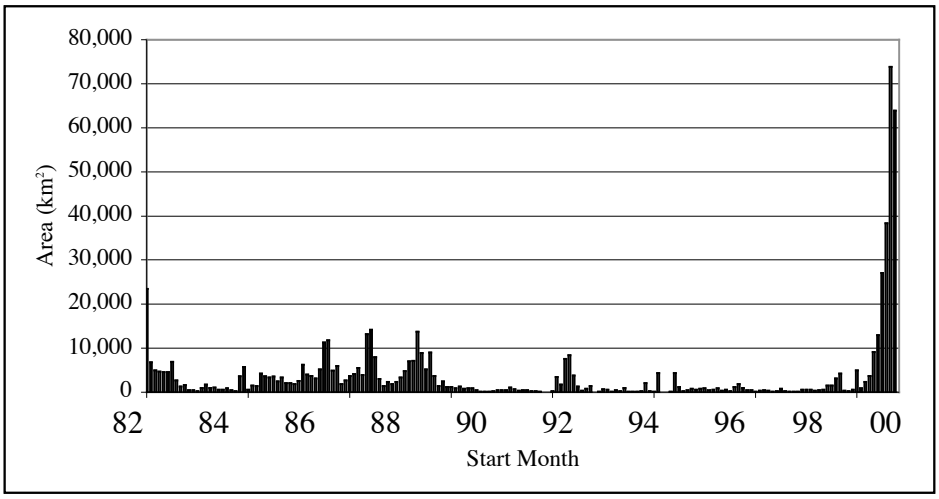

Figure 7. (a) FPAR–LO event in Norway from 1992-1993, showing suspected climate and pollution impacts on vegetation greenness, (b) FPAR–LO event in India in 1998-99, showing reported drought and heat wave impacts on vegetation greenness, (c) FPAR–LO event in eastern Russia in 1987 showing reported forest fire impacts on vegetation greenness, (d) FPAR–LO event on the Siberian Plateau in 1999 showing suspected fire and insect outbreak impacts on vegetation greenness. Data presentation in panels is described as in Figure 1.